Comparison of a Novel Modified PLA/HA Bioabsorbable Interference Screw With Conventional PLGA/β-TCP Screw

Effect on 1-Year Postoperative Tibial Tunnel Widening in a Canine ACLR Model

Chuan Jiang,* PhD, Huaming Peng,* MMed, Yang Sun,† PhD, Sicheng Xu,* MMed, Weiping Li,* BMed, Yucheng Huang,† BMed, Dong Xiang,† MS, Xiaoshan Fan,† PhD, Jinzhong Zhao,‡¶ MD, Chaobin He,§¶ PhD, and Bin Song,*‖¶ PhD
Investigation performed at the Sun Yat-sen Memorial Hospital, Sun Yat-sen University, Guangzhou, People's Republic of China

Background: Tibial bone tunnel widening (TW) is a common postoperative phenomenon after anterior cruciate ligament reconstruction (ACLR).

Purpose: To compare the physical, biomechanical, osteoinductive, and histological characteristics of 2 fabricated bioabsorbable interference screws: (1) a modified poly(L-lactide-*co*-D, L-lactide) and hydroxyapatite (mPLA/HA) screw and (2) a poly(L-lactide-*co*-glycolide) and β-tricalcium phosphate (PLGA/β-TCP) screw; and to evaluate the effect of the PLA/HA screw on ameliorating postoperative TW in a canine ACLR model.

Study Design: Controlled laboratory study.

Methods: In vitro, the physical and biomechanical properties of the mPLA/HA and PLGA/β-TCP screws were tested. The osteoinductive activity of the screws was studied by cell experiments. In vivo, ACLR was performed on 48 beagle dogs, divided into the mPLA/HA group and the PLGA/β-TCP group. The femoral and tibial ends of the graft were both fixed with screws. Six animals in each group were sacrificed after live computed tomography (CT) scanning at 1, 3, 6, and 12 months postoperatively. For six knee samples of each group, three knee samples underwent biomechanical testing, and 1 of them, along with the other 3 samples, underwent micro-CT and histological examination to evaluate tibial TW.

Results: The mPLA/HA screw exhibited better particle dispersion, bending strength, desirable self-locking effect, and optimized degradation behavior both in vivo and in vitro. Histologically, the mPLA/HA screw had comparative osteoinductive activity. There was good screw-bone integration using the mPLA/HA screw, while most fibrous scar healing was in the PLGA/β-TCP group. There were significant differences between the mPLA/HA and PLGA/β-TCP groups in tibial bone tunnel diameter at the screw body (6 months postoperatively: 5.09 ± 0.44 vs 7.12 ± 0.67; 12 months postoperatively: 4.83 ± 0.27 vs 6.23 ± 0.56; $P < .01$ for both) and the screw tail (6 months postoperatively: 4.84 ± 0.28 vs 5.97 ± 0.73; 12 months postoperatively: 4.77 ± 0.29 vs 5.92 ± 0.56; $P < .01$ for both).

Conclusion: Compared with the PLGA/β-TCP screw commonly used in clinics at present, the mPLA/HA screw had comparative biosafety and mechanical properties, satisfactory biomechanical properties, and osteoinductive activity in vivo and in vitro. It effectively ameliorated the postoperative tibial TW in a canine ACLR model and increased the quality of screw-bone integration.

The Orthopaedic Journal of Sports Medicine, 12(10), 23259671241271710
DOI: 10.1177/23259671241271710

Clinical Relevance: The good mechanical and biological properties of the mPLA/HA screws may provide an option to reduce the incidence of complications after ACLR.

Keywords: interference screw; polylactide; hydroxyapatite; tibial tunnel widening; anterior cruciate ligament reconstruction

Bioabsorbable screws in anterior cruciate ligament (ACL) reconstruction (ACLR) have comparable fixation strength[23] with metal screws and good screw-bone integration. Other advantages include little graft cutting during insertion and less radiologic visualization interference.[25,26,35] However, bioabsorbable screws still have some problems that need to be addressed in clinical applications, such as less connection with the bone tunnel,[15] insufficient osteoinductive effects,[31] and inappropriate degradation rate,[16] which may lead to bone tunnel widening (TW) after ACLR.

TW is a well-recognized postoperative phenomenon.[11,21] Studies have shown that the estimated incidence of TW after ACLR using autologous tendons is 25% to 100% in the femoral tunnel and 29% to 100% in the tibial tunnel.[2] The potential clinical impact of TW is that in revision ACLR, excessive TW may not only lead to insufficient bone mass to create new bone tunnels but also prevent the graft from obtaining firm compression fixation in the femoral and tibial tunnels, leading to graft loosening and potential knee instability and ultimately leading to revision failure.[28,32,34] With the increasing number of ACLR procedures performed in recent years, the percentage of revision surgeries can also be predicted to increase yearly.[14] Therefore, how to effectively avoid the occurrence of TW is a foreseeable and realistic problem with important clinical significance.

The causes of TW are mainly biological and mechanical in nature.[6,12,31] The insufficient biomechanical properties of traditional bioabsorbable screws and biological activity around grafts and screws are considered to be one of the possible main causes of TW.[31] Nowadays, the bioabsorbable screws commonly used in the clinic are mostly made of materials such as poly-L-lactic acid (PLLA),[5] poly-L-lactide/glycolide acid (PLGA),[39] tricalcium phosphate (TCP),[35] and hydroxyapatite (HA).[20] These materials have different advantages in biomechanical properties, biocompatibility, and osteogenic activity.

In the present study, a modified bioabsorbable interference screw was fabricated based on poly(L-lactide-*co*-D, L-lactide) (mPLA) and HA (mPLA/HA screw). In vitro and in vivo biomechanical, imaging, and histological assessments were carried out for the mPLA/HA screw in comparison with a fabricated screw modeled on one of the most widely used conventional interference screws, made of PLGA and β-TCP (PLGA/β-TCP screw). We hypothesized that the mPLA/HA screw would have comparable biomechanical properties, satisfactory osteoinductive properties, and optimized degradation behaviors with the PLGA/β-TCP screw and that it would effectively ameliorate TW in a canine ACLR model.

METHODS

The protocol for this study received ethics committee approval, and the study was performed from April 2020 following the Guide for the Care and Use of Laboratory Animals.[19] In the canine ACLR arm of the study, we compared the experimental group (mPLA/HA group; n = 6) and the control group (PLGA/β-TCP group; n = 6). Observation endpoints were set at 1, 3, 6, and 12 months postoperatively.

Fabrication of the Interference Screws

The experimental (mPLA/HA) group interference screws were made of 80 wt% PLA (L-lactide-*co*-D, L-lactide molar ratio 4:1) and 20 wt% HA. The PLA/HA composites were fabricated by dispersing HA into PLA in chloroform through an ultradispersity technique, followed by

¶Address correspondence to Bin Song, PhD, Department of Orthopedics, Sun Yat-sen Memorial Hospital, 107 West Yanjiang Road, Guangzhou 510120, People's Republic of China (email: songbin3@mail.sysu.edu.cn); Jinzhong Zhao, MD, Department of Sports Medicine, Shanghai Sixth People's Hospital, Shanghai Jiao Tong University, 600 Yishan Road, Shanghai 200233, PR China (email: zhaojinzhong@vip.163.com); and Chaobin He, PhD, Department of Materials Science & Engineering, National University of Singapore, 9 Engineering Drive 1, 117576 Singapore (email: msehc@nus.edu.sg).

*Department of Orthopedics, Sun Yat-sen Memorial Hospital, Sun Yat-sen University, Guangzhou, People's Republic of China.

†Shenzhen Corliber Regenerative Materials Laboratory, Shenzhen, People's Republic of China.

‡Department of Sports Medicine, Shanghai Jiao Tong University Affiliated Sixth People's Hospital, Shanghai, People's Republic of China.

§Department of Materials Science & Engineering, National University of Singapore, Singapore.

‖Department of Joint Surgery & Sports Medicine, The Sixth Affiliated Hospital of Sun Yat-sen University, Guangzhou, People's Republic of China.

C.J. and H.P. contributed equally to this article.

J.Z., C.H., and B.S. contributed equally to this article and are considered co–corresponding authors.

Final revision submitted January 9, 2024; accepted February 12, 2024.

One or more of the authors has declared the following potential conflict of interest or source of funding: Financial support for this study was received from the Guangdong Basic and Applied Basic Research Foundation (2021A1515012337, 2019A1515011684), the National Natural Science Foundation of China (82172416, 81802172), and the Natural Science Foundation of Guangdong Province (2022A1515010215). AOSSM checks author disclosures against the Open Payments Database (OPD). AOSSM has not conducted an independent investigation on the OPD and disclaims any liability or responsibility relating thereto.

Ethical approval for this study was obtained from the Suzhou Zhen Hu Medical Technology (ref No. ECSZZHYL-19101102).

precipitation in methanol and vacuum drying. The control (PLGA/β-TCP) group interference screws were made of 70 wt% PLGA and 30 wt% β-TCP. The PLGA/β-TCP composites were prepared similarly to PLA/HA composites.

For the mPLA/HA screw, small granules of PLA/HA composites were extruded at 180°C to form a thick cylindrical form, or billet, 14 mm in diameter (designated as "extruded billet"). The extruded billet was forged at 90°C into a cylindrical thinner billet 10 mm in diameter (designated as "molded billet") without fibrillation by compression molding. The molded billet was subsequently carved on a lathe into an mPLA/HA screw. Next, the PLGA/β-TCP screws were directly fabricated by extruding small granules of PLGA/β-TCP composites at 150°C into a screw melt-injection mold.

For both groups, the finished screws were 5 mm in diameter and 12 mm in length.

Physical and Biomechanical Characteristics

HA Particle Size Measurement and Dispersity in Standing Solution. A small piece of material was cut off of a screw and dissolved in a 15-mL centrifugation tube with 5 mL dichloromethane (1 mg/mL). An intense light was placed behind the centrifugation tube for observation purposes, and changes in the solution were recorded at different standing time points. Transmission electron microscopy (TEM) (FEI Titan 80-300 scanning TEM) observation was conducted under an acceleration voltage of 80 kV. A single droplet of the homogeneous solution prepared for standing observation was placed onto a TEM copper grid, where HA particle size and dispersity in dry solid form could be observed. Dynamic light scattering was utilized to measure the particle size in the homogeneous solution at 25°C on a Brookhaven BI-200SM multiangle goniometer equipped with a Brookhaven BI-APD avalanche photodiode detector (the light source was a 35-mW He-Ne laser emitting vertically polarized light of 632.8-nm wavelength).

In Vitro Mechanical Verification of Screw Fixation Effect and Strength. To verify the clinical usability of the screws, we first conducted in vitro mechanical validation tests on the screws, including testing the fatigue properties in ligament fixation, the bending properties of the molded billets, and the ligament pullout force during accelerated degradation. Details of the testing methods are provided in the Supplemental Material (available separately).

Accelerated Degradation. To understand the changes in molecular properties of the screw from the beginning to the completion of degradation, we performed an accelerated degradation test. Briefly, the screw sample was weighed and placed in a sealed centrifugation tube with the addition of phosphate-buffered saline (PBS) buffer solution and then kept in an oven at 70°C. At the designed time point, 3 degraded samples from each group were removed, carefully rinsed with pure water, and dried in a vacuum oven at 80°C for 12 hours for further use. After degradation, the sample mass was recorded on an electronic balance. After that, a small piece of material was taken from the sample for morphology observation by a scanning electron microscope (SEM). The rest underwent a polymer collection process for molecular weight and inherent viscosity tests. Gold was sputtered on SEM observation samples. The polymer was collected by a dissolution-centrifugation process. Polymer inherent viscosity was measured on a Ubbelohde viscometer using chloroform as the solvent. The molecular weight of the collected polymer was measured by gel permeation chromatography in chloroform.

Measurement of Screw Swelling Properties. To measure the swelling properties, 3 mPLA/HA screws and 3 PLGA/β-TCP screws were immersed in PBS solution at 37°C for 30 days. The screw head diameter and screw body diameter were measured every other day.

In Vitro Cell Experiments

Cell Culture and Proliferation. Rabbit bone marrow mesenchymal stem cells (RBMSCs) and mouse embryonic osteoblast precursor cells (MC3T3E1), purchased from the Cell Bank of the Chinese Academy of Sciences, were cultured in the complete culture mediums made of Dulbecco's modified Eagle medium added with 10% fetal bovine serum and 1% penicillin. Cells were incubated in the complete medium (5% CO2; 37°C).

The composite samples of the mPLA/HA screw and PLGA/β-TCP screw were prepared into wafers by a dissolution-casting method, which was sterilized for cell culture. Then, the 2 groups of samples were placed in 96-well plates, and the RBMSCs and MC3T3E1 were respectively seeded on the surface with a proper density. Another group of RBMSCs and MC3T3E1 without any composite samples was also cultured as a control group. Next, cell proliferation was examined using Cell Counting Kit 8 (Dojindo Molecular Technology) following the manufacturer's instructions at 1, 3, 5, and 7 days after incubation.

Real-Time Polymerase Chain Reaction Analysis and Cytological Staining Analysis. The expression of the osteogenesis-related mRNA (osteopontin [OPN], osteocalcin [OCN], collagen type 1 [Col-I], and alkaline phosphatase [ALP]) of MC3T3E1 osteoblasts was detected by real-time polymerase chain reaction after incubation for 3 and 7 days for comparison among the mPLA/HA group, PLGA/β-TCP group, and a control group (β-actin was used as a quantitative control for RNA levels). The sequences of the primers are listed in Supplementary Tables S1 and S2 (available separately). Also, alizarin red staining was performed on the culture medium of the 3 groups on days 14 and 21, and the distribution of calcium and phosphorus in the culture medium was observed.

In Vivo Experiments

ACLR in a Canine Model. A total of 48 healthy beagle dogs (18 months old, weight, 10.0-15.0 kg, male) were selected to establish the unilateral ACLR model on the left hind legs. The canine model was established according to a previous study.[9] First, a skin section was made along the posterior side of the distal tibia, and the flexor

digitorum longus tendon was found, then transected and woven into ligament grafts, and the incision was sutured. Then, the articular cavity of the left knee was exposed by medial parapatellar arthrotomy and dislocation of the patella, followed by transection of the ACL. A 1.5 mm–diameter bone tunnel was drilled into the femur and the tibia according to the position of the native ACL insertion, and a 4.8-mm hollow drill was used for TW. The autograft was then pulled through both bone tunnels. By random assignment, 2 mPLA/HA screws (mPLA/HA group; n = 24) or 2 PLGA/β-TCP screws (PLGA/β-TCP group; n = 24) were inserted into the tibial and femoral tunnel by a screwdriver with the graft stretched, and the incisions were sutured layer by layer. The dogs were cared for in the same environment.

Postoperative CT Imaging. Each animal group underwent computed tomography (CT) imaging under anesthesia at 3 days and 1, 3, 6, and 12 months postoperatively. For each group of animals, the status of the knee ligament was observed and recorded intraoperatively, postoperatively, and at the time of sampling.

Biomechanical Analysis. Six dogs were sacrificed for left hind knee samples at each postoperative time point (1, 3, 6, and 12 months). In each group, 3 knees underwent a pullout test and degradation test. For the pullout test, the ends of the femur and tibia of each sample were fixed in clamps, and a 5-N preload was applied. Then, a tensile load was applied at a speed of 5 mm/minute until the ligament was broken or pulled out from the bone tunnel. The circumference of the ligament of the specimens of both groups was recorded, together with the load-displacement curve, failure load, and failure mode. The ligament cross-sectional area, displacement, tensile strength, and stiffness were obtained by calculation.

To investigate the material degradation behavior in vivo, the screw implanted in the femur of each sample was used to measure molecular weight and inherent viscosity at each endpoint.

Imaging, TW, and Bone Mass Analysis. One of the samples that underwent biomechanical testing also underwent micro–CT scanning along with the remaining 3 knee samples. The binarized images were analyzed with Skyscan software (Skyscan 1176; Bruker). The bone tunnel measurements of both groups were evaluated by analyzing the micro-CT imaging data. To more intuitively reflect the impact of the screws on the bone tunnels and reduce possible bias caused by irregular bone tunnels, we first selected a cross-sectional image perpendicular to the screw axis on micro-CT, choosing the screw body and screw tail layers. Then, we determined the longest diameter (d_1) and the shortest diameter (d_2) of the bone tunnel on these layers, as well as d_3 and d_4, which bisect the angles formed by d_1 and d_2. The diameter of the bone tunnel at the screw body or tail was calculated as $d = (d_1 + d_2 + d_3 + d_4)/4$ (Figure 1).

Based on the 3-dimensional reconstructed images, a cylindrical region of interest parallel to the tibial bone tunnel was selected to measure the bone volume/total volume (BV/TV) of both groups.

Histological Analysis. After micro-CT imaging, the tibial part of each sample was prepared into paraffin sections and stained with the hematoxylin and eosin and Masson-Goldner staining. Slide observation and photographs were performed under a light microscope (Eclipse Ni-U; Nikon). The Lane-Sandhu scoring system[37] was applied to evaluate the screw-bone integration under Masson-Goldner staining.

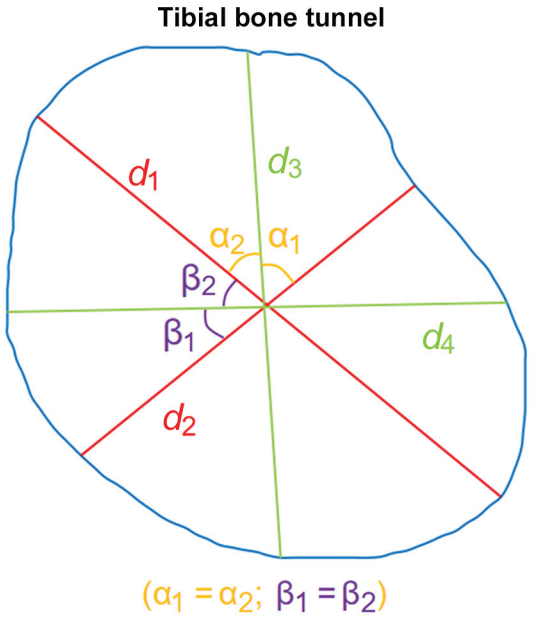

Figure 1. Schematic diagram for measuring the diameter of the tibial bone tunnel, calculated as $(d_1 + d_2 + d_3 + d_4)/4$.

Statistical Analysis

Data were recorded as mean ± standard deviation. The differences between the mPLA/HA and PLGA/β-TCP groups were determined by t test or 1-way analysis of variance. Statistical significance was set at $P < .05$. All analyses were conducted with SPSS software for Windows (Version 20.0; IBM).

RESULTS

Particle Dispersity of the Polymer Composites

The standing solutions of both screw groups exhibited homogeneity right after preparation (0 minutes), and no impurities or big particles were visible. After 10 minutes of standing, obvious precipitation was found at the tube bottom in the PLGA/β-TCP group. After 35 minutes of standing, more precipitation was found at the tube bottom of the PLGA/β-TCP group, and the supernatant turned transparent. However, no precipitation was observed in the mPLA/HA group, and the solution remained milky and uniform (Figure 2A). The solution observation indicated that the particle dispersion was more stable in the mPLA/HA group.

Inorganic particles were well dispersed in the composites of both groups (Figure 2B). The HA particles in the

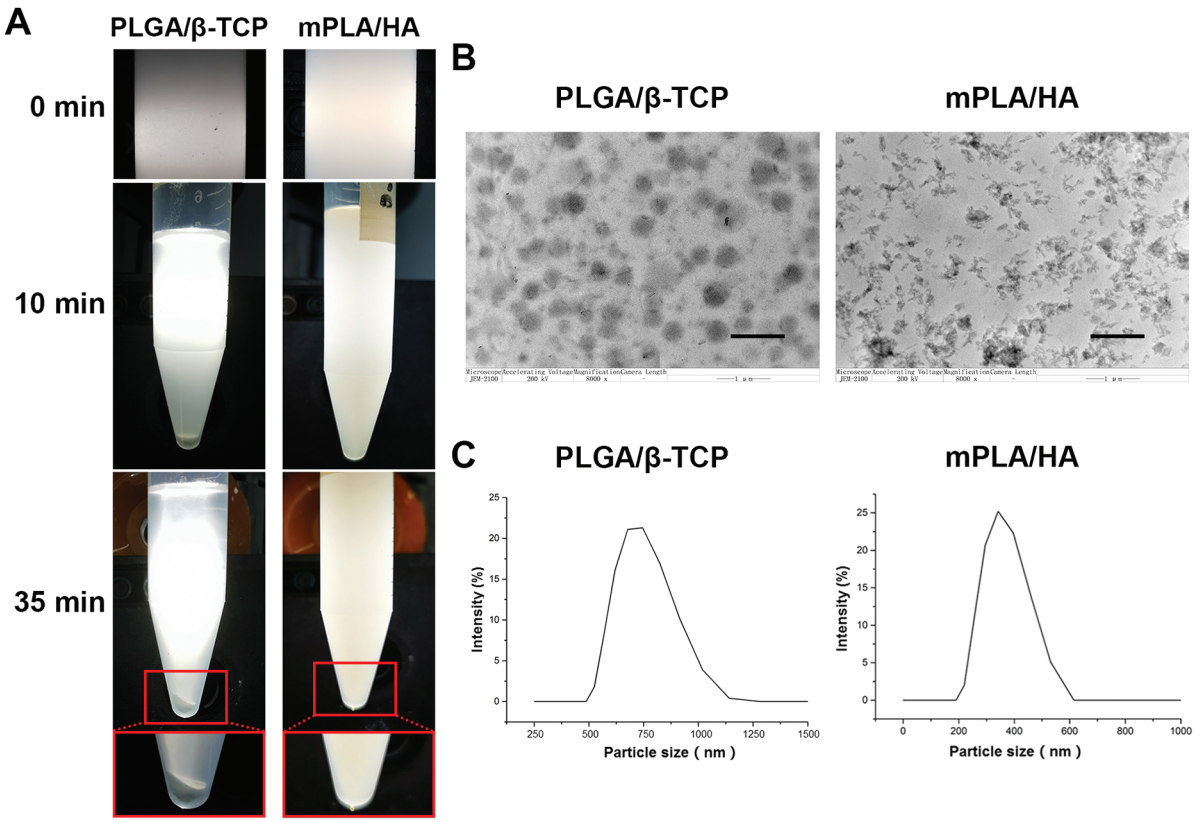

Figure 2. Results of standing solution observation for the mPLA/HA and PLGA/β-TCP groups. (A) The dispersion and precipitation of particles at different standing time points in dichloromethane solution. (B) Transmission electron microscopy observation of the HA particles in the mPLA/HA group and the β-TCP particles in the PLGA/β-TCP group (scale bar: 1 μm). (C) Particle size measurement according to dynamic light scattering in the dichloromethane solution.

mPLA/HA group were of small aggregates around 200 nm, while the β-TCP particles in PLGA/β-TCP group were of spherical shape, mostly around 400 nm. The particle size of the mPLA/HA screw composites and PLGA/β-TCP screw composites distributed as a single peak at about 390 and 750 nm in dichloromethane solution, respectively (Figure 2C), indicating ideal uniformity of particle dispersion in both groups and finer particle dispersity in the mPLA/HA group.

Ligament Pullout Fixation Properties

Under a 50- to 80-N load, no failure was found between the nylon rope and the mPLA/HA screws after 10,000 cyclic loads, and the mean displacement was 0.5 ± 0.4 mm. The PLGA/β-TCP screws had a more significant displacement of 2.8 ± 1.2 mm ($P < .05$) (see Supplementary Figure S1D, available separately). The subsequent static tensile strength tests showed that the mPLA/HA screws had an ultimate load of 141 ± 8 N, with an ultimate displacement of 20.2 ± 3.6 mm, compared with an ultimate load of 139 ± 9 N and ultimate displacement of 19.7 ± 2.0 mm for the PLGA/β-TCP screws, with no significant difference between the 2 groups (Supplementary Figure S1D).

Accelerated Degradation In Vitro

For both the mPLA/HA and PLGA/β-TCP groups, no material corrosion on the surface was visible until 1 day of accelerated degradation. At 3 days, both groups started to exhibit surface material corrosion (Figure 3A); this coincided with the time point of mass loss (Figure 3D). At 7 days of accelerated degradation, inorganic particles were exposed due to material corrosion arising from degradation. When samples were collected and dried after 14 days of accelerated degradation, screws in the mPLA/HA group were able to maintain their shape but needed to be handled carefully to avoid collapse, while the PLGA/β-TCP screws were completely crushed (Supplemental Figure S2). SEM observation of the mPLA/HA screws showed obvious exposure of inorganic particles on the material surface (Figure 3, B and C). Screws in the PLGA/β-TCP group were crushed into a powder that could not go through SEM observation.

No apparent mass loss occurred at 6 hours and 1 day of accelerated degradation in the 2 groups, and both started to lose mass at around day 3 and experienced fast mass loss from day 7 to day 14. In addition, a noticeable drop in inherent viscosity and molecular weight were observed in both groups at day 1. After 3 days, the inherent viscosity retention rate reached around 10%, and the molecular

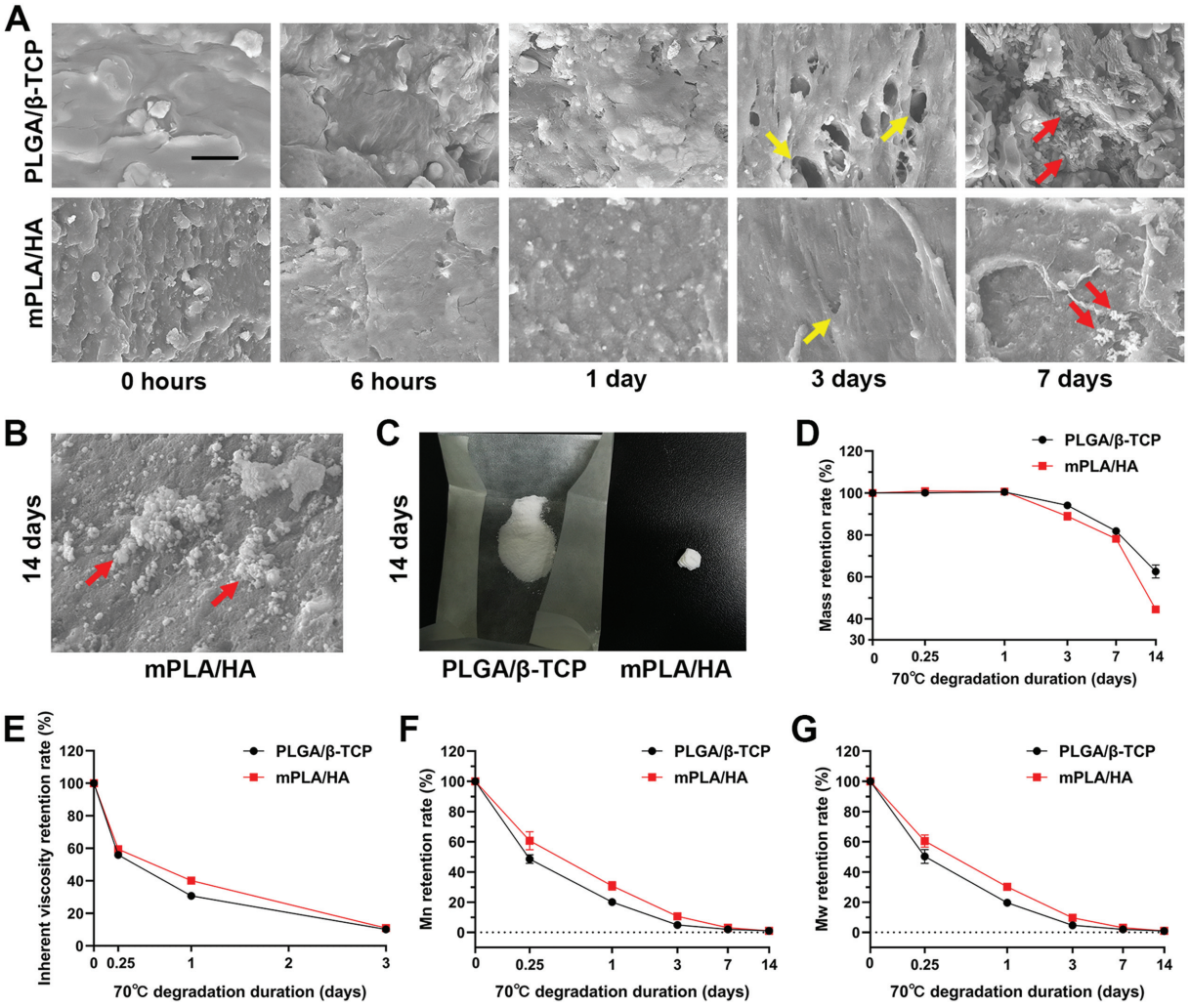

Figure 3. (A) Scanning electron microscope (SEM) observation of both screws groups after 0 hours, 6 hours, 1 day, 3 days, and 7 days of degradation (scale bar: 10 μm). The yellow arrows show the surface material corrosion. The red arrows show the inorganic particles exposed due to material corrosion. (B) SEM observation of a mPLA/HA screw after 14 days of accelerated degradation, showing obvious exposure of inorganic particles (red arrows) on the material surface. (C) After 14 days of accelerated degradation, the mPLA/HA screw was able to maintain its shape but needed to be handled carefully to avoid being crushed, while the PLGA/β-TCP screw had been crushed into powder. (D-G) The mass, inherent viscosity, and molecular weight (Mn and Mw) retention rate of both screws at each endpoint. Error bars represent SDs.. Mn, number-mean molecular weight; Mw, weight-mean molecular weight.

weight retention rate reached below 3% at day 7 for both groups. In terms of accelerated degradation behaviors, the mPLA/HA screw was basically equivalent to the PLGA/β-TCP screw (Figure 3, D-G).

Bending Properties of the Molded Billets

SEM observation indicated that the molded billets of the mPLA/HA screw had a highly oriented alignment of molecular chains compared with the PLGA/β-TCP screw, which was also shown by the small-angle X-ray scattering diffraction patterns (Figure 4, A and B). The molecular chain alignment of the mPLA/HA screws indicated a large improvement in the strength of the materials compared with conventional materials, providing a guarantee for sufficient mechanical strength in the clinical application of the screws.

Under degradation at 37°C in PBS solution, the mPLA/HA screw billets showed higher bending strength, yield strength, and flexural modulus, while the PLGA/β-TCP screw billets showed lower bending properties comparable with the cortical bone (Figure 4, C-E).

The bending strength of the mPLA/HA screw billets remained above that of young cortical bone within 5 months of real-time degradation (Figure 4C). Even though the bending strength decreased at 6 months of degradation, it was still equivalent to that of osteoporosis. At the same time, its yield strength was always greater than

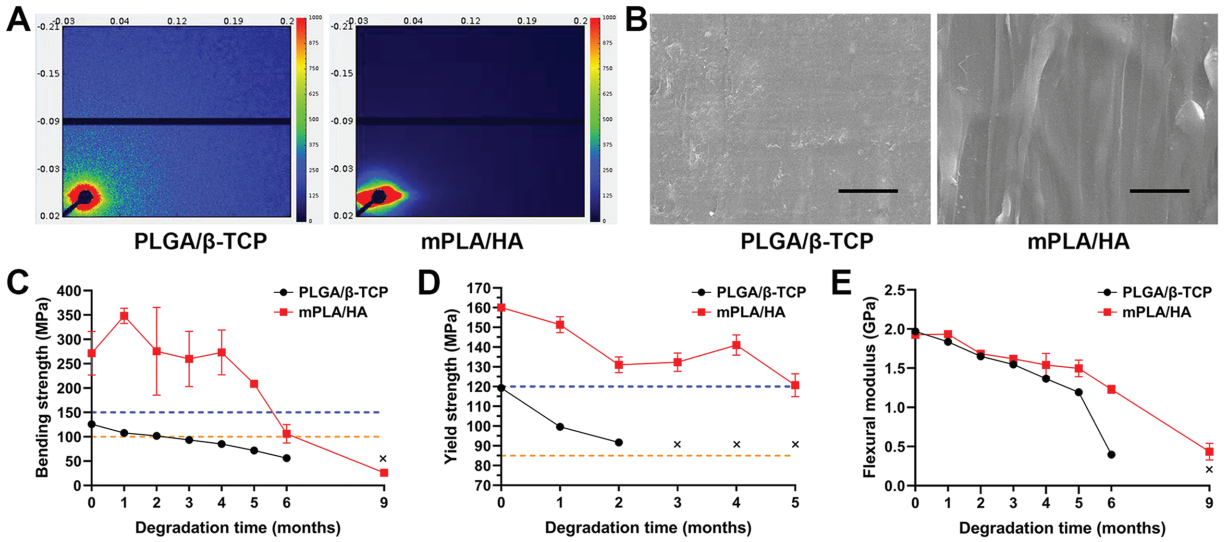

Figure 4. The bending properties of the molded billets. (A) Small-angle X-ray scattering diffraction patterns and (B) scanning electron microscope observation (length of the scale is 10 μm) of mPLA/HA screw molded billets and PLGA/β-TCP screw injection billets. (C-E) Bending property changes with degradation duration, where the blue and yellow dashed lines represent reference values of bending properties of cortical bone in young adults and osteoporosis patients, respectively. Xs indicate areas where data could not be presented on the graph because degradation made it difficult to complete the test or that the test results could not be calculated. Error bars represent standard deviations.

cortical bone in young people within 5 months and much greater than that in patients with osteoporosis (Figure 4D). In addition, the flexural modulus of the mPLA/HA screw had a good retention rate within 6 months of degradation. Although the flexural modulus absolute value was less than that of human cortical bone (about 6 GPa), the 2 values were in the same order of magnitude, which means that the mPLA/HA screw can stably play a role in internal fixation during bone healing and will not lead to a stress-shielding effect (Figure 4E).

Ligament Pullout Force During Accelerated Degradation

During in vitro accelerated degradation, the ligament pullout force of the 2 groups decreased continuously, almost disappearing at 7 days (Supplementary Figure S3). However, the ligament pullout force of the mPLA/HA group was significantly higher than that of the PLGA/β-TCP group on day 4 of degradation ($P = .002$). There were no significant group differences at the other degradation time points.

Screw Swelling Properties

As time passed, the head diameter and body diameter of the mPLA/HA screw placed in the PBS buffer increased continuously and reached a plateau value at about 30 days. In contrast, the head diameter and body diameter of the PLGA/β-TCP screw did not change significantly (Supplemental Figure S4).

Cell Proliferation Promotion and Osteogenesis

Compared with the PLGA/β-TCP group, the mPLA/HA group exhibited more cell proliferation and a faster proliferation rate, but the level was lower than that of the control group (Figure 5, A and B). For gene expression related to osteogenic differentiation of RBMSCs, the expression of OCN, ALP, and Col-I was higher in the PLGA/β-TCP group. But for the osteoblast MC3T3E1, the expression of OPN, OCN, and ALP in the mPLA/HA group was significantly higher than that in the PLGA/β-TCP group, while the expression of Col-I in the PLGA/β-TCP group was higher. In addition, the expression of OPN in the mPLA/HA group was higher than that in the blank control group (Figure 5, D-E). Results demonstrated that mPLA/HA screw material can effectively promote the process of osteogenic metabolism of osteoblasts and is more conducive to osteogenesis.

In alizarin red staining of the medium on days 14 and 21, the calcium and phosphorus concentration in the medium of RBMSCs in the mPLA/HA group was higher and more evenly distributed than in the PLGA/β-TCP group (Figure 5C). In the MC3T3 medium, the calcium content in the non–material covered area of the medium in the mPLA/HA group was higher (deep red stained region). The findings indicated that the mPLA/HA screw material promoted osteoblast osteogenesis metabolism and produced more calcium than the PLGA/β-TCP screw material, which was more conducive to osteogenic mineralization.

Screw Performance in the Canine ACLR Model

The ligament reconstruction was intact and the range of joint motion was normal in the canine ACLR model

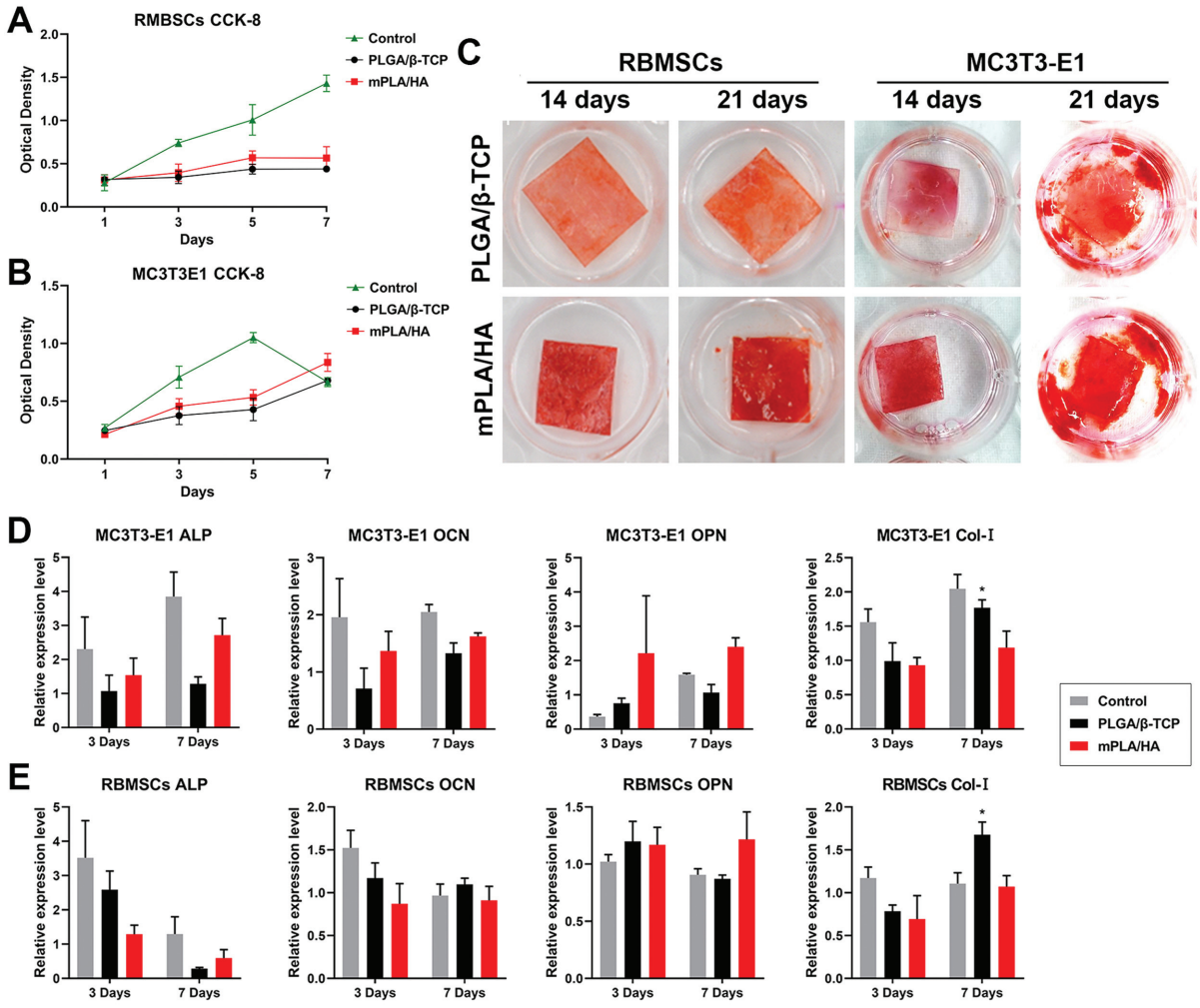

Figure 5. The properties of promoting cell proliferation and osteogenesis of the screws. (A and B) Optical density of (A) rabbit bone marrow mesenchymal stem cells (RBMSCs) and (B) mouse embryonic osteoblast precursor cells (MC3T3E1) seeded on the different groups after 1, 3, 5, and 7 days using Cell Counting Kit 8 (CCK-8). (C) Alizarin red staining of the culture medium of RBMSCs and MC3T3E1, in which the calcium was stained orange or red. (D-E) The mRNA level of the osteogenic-related genes expressed by the RBMSCs and MC3T3E1 seeded on samples of different groups at 3 and 7 days. Error bars in all of the graphs represent standard deviations. ALP, alkaline phosphatase; Col-I, collagen type 1; OCN, osteocalcin.

(Supplemental Figure S5). At 1, 3, 6, and 12 months postoperatively, in the biomechanical pullout test, the ultimate failure mode of both groups was that of graft rupture under increasing tensile load as opposed to the graft's dislodging the bone tunnel together with the screw. There were no significant differences in failure load, tensile strength, or stiffness between the 2 groups (Figure 6, A-D). In addition, the inherent viscosity retention rate and molecular weight retention rate of both screws continued to drop within 6 months and reached a plateau after 6 months. During degradation, the inherent viscosity retention rate and molecular weight retention rate of mPLA/HA screws were always higher than those of PLGA/β-TCP screws (Figure 6, E-G).

TW and Bone Mass on CT Imaging and Micro-CT of the Tibial Samples

The CT scans showed that for both screw groups, the connection between the screw and bone tunnel was mostly tight within 3 days postoperatively. All screws showed some enlargement at 1 month postoperatively. However, the bone tunnel around the screw interface of the PLGA/β-TCP group showed further widening at 3, 6, and 12 months, with some local arcs of osteolysis on both sides of the screw. In contrast, the bone tunnels in the mPLA/HA group tended to decrease enlargement by 6 and 12 months postoperatively, and the bone tunnel had more connection with the screw at the interface (Supplementary Figure S6).

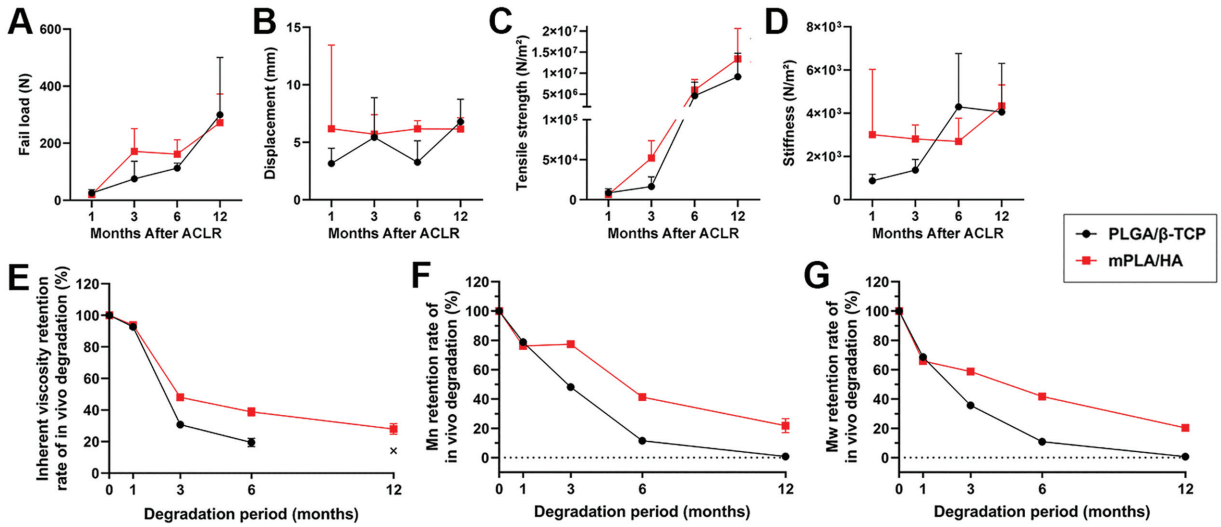

Figure 6. The biomechanical results at each time point after anterior cruciate ligament reconstruction (ACLR) in a canine model. (A-D) The ligament pullout force test results after real-time degradation. There was no ligament detachment in either screw group. Error bars represent SDs. (E-G) The inherent viscosity retention rate, number (Mn), and weight (Mw) mean molecular weight retention rate after real-time degradation in vivo. Since the PLGA/β-TCP screws had been fragmented at 12 months, it was difficult to sample from the tissue, and we could not obtain enough material for the inherent viscosity test (indicated by X).

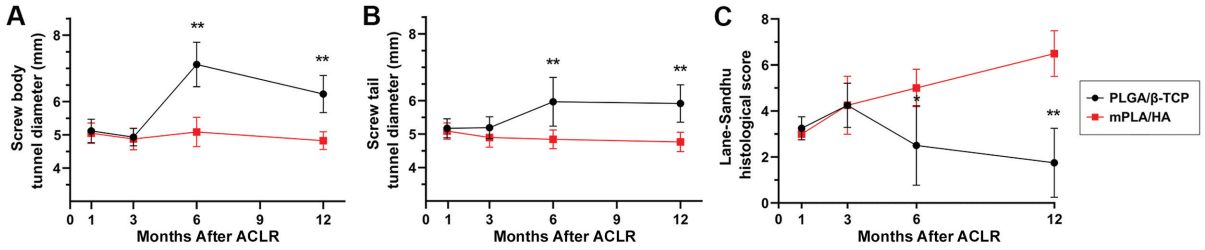

Figure 7. (A-B) Postoperative changes in the mean width of the tibial bone tunnel at the (A) screw body and (B) screw tail in the mPLA/HA and PLGA/β-TCP groups. (C) The Lane-Sandhu scores of tibial bone tunnel healing in Masson-Goldner staining in both groups. Error bars represent SDs. Significant group differences: $^{**}P < .01$.

Regarding the measurement of the tibial bone tunnel diameter using micro-CT, the tunnel diameter of the PLGA/β-TCP group became wider after 3 months postoperatively, and it mostly did not show healing but still showed enlargement of the bone tunnel at 12 months. On the contrary, the diameter of the mPLA/HA group expanded little and showed good healing tendency over time. There were significant differences between the mPLA/HA and PLGA/β-TCP groups in tibial bone tunnel diameter at both the screw body (6 months postoperatively: 5.09 ± 0.44 vs 7.12 ± 0.67, respectively; 12 months postoperatively: 4.83 ± 0.27 vs 6.23 ± 0.56, respectively; $P < .01$ for both) and the screw tail (6 months postoperatively: 4.84 ± 0.28 vs 5.97 ± 0.73, respectively; 12 months postoperatively: 4.77 ± 0.29 vs 5.92 ± 0.56, respectively; $P < .01$ for both) (Figure 7). Moreover, there was high-density new bone formation around the mPLA/HA screw, and the cortical bone healed well, demonstrating that it had the capability of promoting bone healing. Both screws had gradually fragmented at different degrees, but after 12 months of degradation in vivo, the mPLA/HA screw still maintained its cylindrical shape (Figure 8). Overall, the bone tunnel of the mPLA/HA group showed a tendency of converging or decreasing expansion over time.

Based on the 3-dimensional reconstructed images, there were no significant group differences in BV/TV around the tunnel within 6 months after ACLR, and the BV/TV had decreased significantly by 12 months postoperatively in both groups (Supplemental Figure S7). This is because the composition of the screw material was similar to the bone, which interfered with the bone mass analysis of micro-CT.

Histological Section Analysis of Tibial Samples. Hematoxylin and eosin staining also showed a gap between the screw and the tibial bone tunnel in both groups at 1 month postoperatively, but the gap seemed to become wider in the PLGA/β-TCP group as time passed, while the mPLA/HA group was still small (Figure 9). As shown in the Masson-Goldner staining slices (Figure 10), osteoid tissue and new bone appeared around the screws in the mPLA/HA group at 3, 6, and 12 months, with the bone tunnel

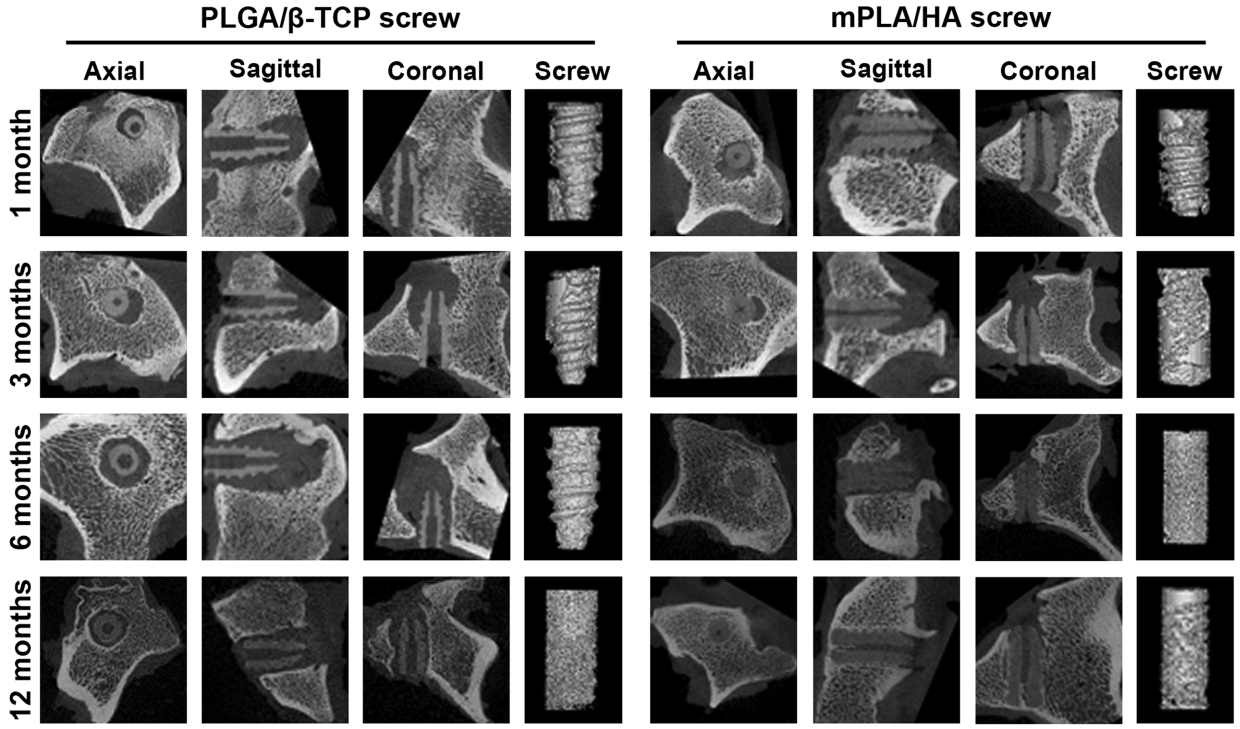

Figure 8. Micro–computed tomographic images of tibial samples from axial, coronal, and sagittal slices and 3-dimensional reconstruction of the screws at each endpoint after anterior cruciate ligament reconstruction. The tibial bone tunnel in the PLGA/β-TCP group mostly widened as time passed after the operation. The tibial bone tunnel width of the mPLA/HA group was maintained and even narrowed in some cases.

finally healed and the cortical bone also recovering well. On the other hand, PLGA/β-TCP screws were gradually fragmented. After fragmentation, little bone tissue grew around the screws.

There was healing filled with fibrous tissue between the screw and the bone tunnel, and there was no sign of recovery of cortical bone (Figures 9 and 10). In addition, with the osteogenic effect, the interface between the screw and tendon or between the graft and bone of the mPLA/HA group were firmly fixed and tightly connected, which provided a good condition for bone-tendon healing. We did not see an obvious inflammatory reaction around the tendon, and there was no significant difference between the 2 groups in the bone-tendon interface.

The Lane-Sandhu histological score (Figure 7C) showed that the effect of promoting bone healing in the mPLA/HA group was equivalent to that in the PLGA/β-TCP group at 1 and 3 months postoperatively. Additionally, at 6 and 12 months postoperatively, the effects of screw-bone integration, cancellous bone healing, and cortical bone healing in the mPLA/HA group were significantly better than those in the PLGA/β-TCP group ($P < .05$).

DISCUSSION

The results of this study showed that the mPLA/HA screw had comparable mechanical properties and equivalent graft fixation strength compared with the PLGA/β-TCP screw. In addition, the mPLA/HA screw was shown to have improved bending strength, optimized degradation behavior, desired swelling properties, and satisfactory osteogenesis-promoting capability. The mPLA/HA screw was also found to promote screw-bone integration and effectively ameliorate TW in a canine ACLR model.

The micromotion of the graft in the tunnel is one of the mechanical factors of TW.[7,27,30] The unstable match, especially among grafts, screws, and tunnel bones, leads to continuous friction at early postoperation.[8,10,13,17] Micromotion can also exacerbate the infiltration of inflammatory joint fluid. It has been demonstrated that high levels of inflammatory cells and inflammatory factors in joint synovial fluid exist long after ACLR.[3,4] The inflammation directly or indirectly stimulates osteoclastogenesis and inhibits osteoblastic activity, causing bone resorption or postoperative osteolysis.[22,36] Thus, the factors mentioned above not only affect tendon-bone healing but also increase the occurrence of osteolysis and bone resorption around screws, which may eventually lead to TW. In this study, the mPLA/HA screw had a self-locking effect between the screw and the bone tunnel because of its particular self-swelling property. Thus, compared with PLGA/β-TCP screws, the diameter of the mPLA/HA screws expanded by about 10%, and the 1-month postoperative CT scans showed a closer connection and better matching in the screw-bone interface. Good matching not only reduces the fretting of the graft in the

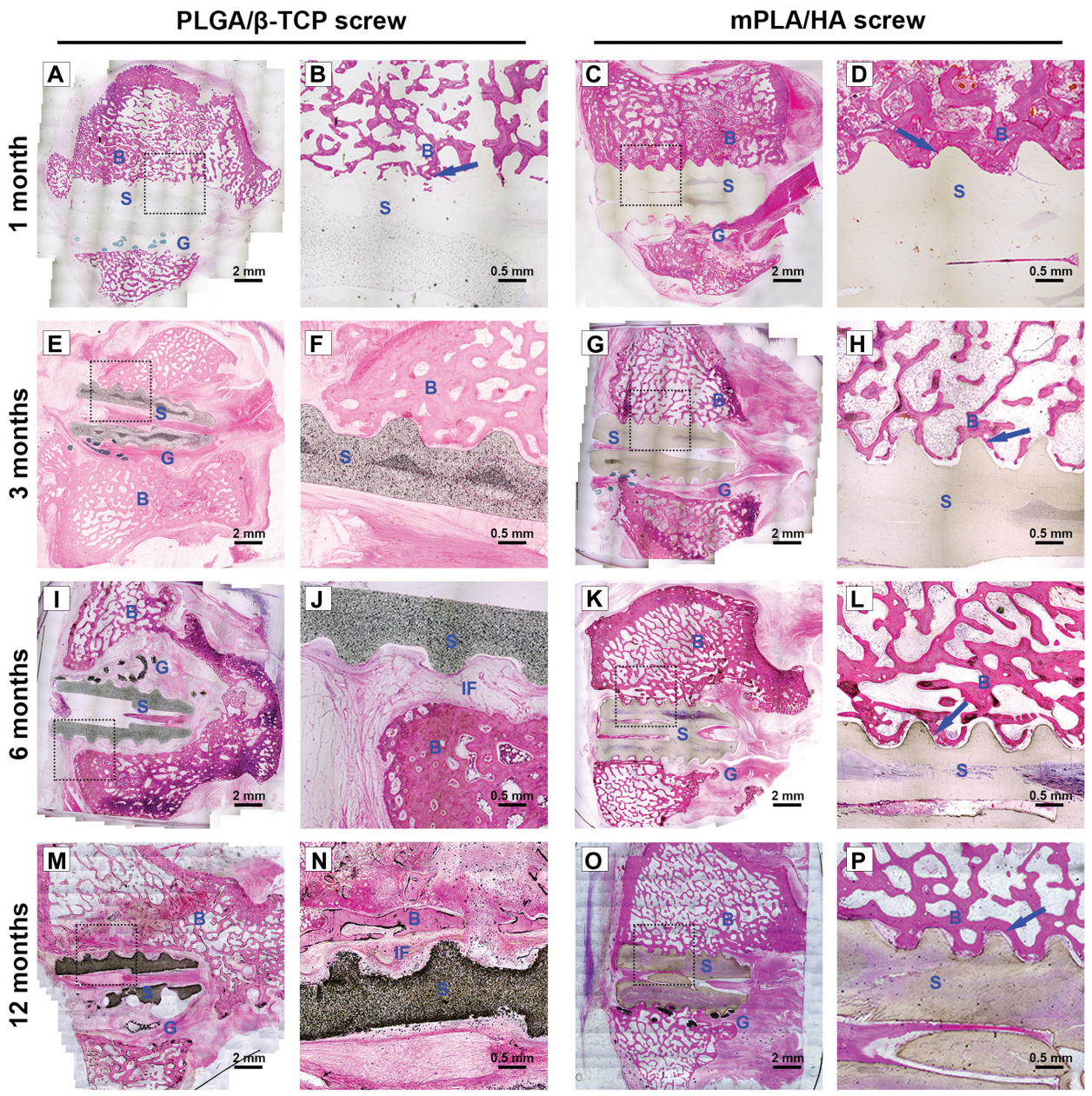

Figure 9. Hematoxylin and eosin–stained slices of the sagittal section of the tibial bone tunnels at 1, 3, 6, and 12 months after anterior cruciate ligament reconstruction in a canine model. (A, C, E, G, I, K, M, O)For each screw group, the images on the right are enlargements of the boxes in the images on the left. (F, J, N) There was a gap between the screw and the bone tunnel at 3, 6, and 12 months postoperatively in the PLGA/β-TCP group. The fibrous tissue was filled in the interface. (D, H, L, P) The interface between the screw and the bone tunnel was still small as time progressed in the mPLA/HA group (arrows). B, bone; G, graft; IF, interface; S, screw.

bone tunnel but also prevents the infiltration of inflammatory joint fluid into the bone tunnel.

The properties of HA materials in promoting osteogenesis, cell adhesion, and proliferation have been widely recognized.[20] Furthermore, it is believed that smaller particle sizes and better dispersion contribute to the endocytosis of HA particles by osteoblasts, which promotes the gene expression of osteoblasts through intracellular reaction and facilitates the induction of osteogenesis.[38] This study demonstrated that HA particles with smaller particle sizes compared with TCP particles showed better promoting osteogenesis in the in situ microenvironment. Likewise, new bone formation between the screw and the bone tunnel was observed in vitro. Thus, mPLA/HA screws may ameliorate the TW by facilitating screw-bone integration.

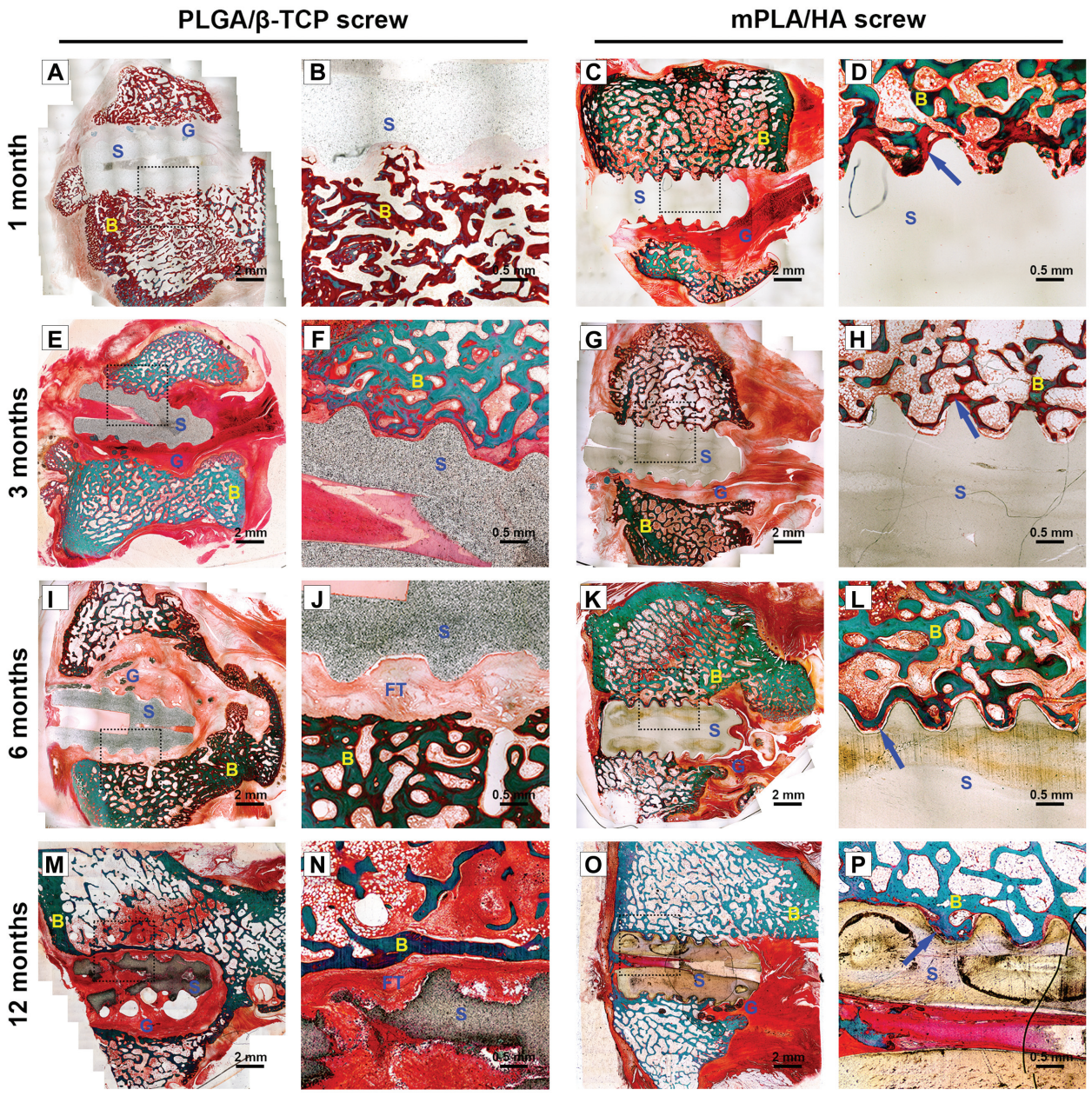

Figure 10. Masson Goldner–stained slices of the sagittal section of the tibial bone tunnels at 1, 3, 6, and 12 months after anterior cruciate ligament reconstruction. For each screw group, the images on the right are enlargements of the boxes in the images on the left. (J, N) There was healing filled with fibrous tissue in the interface between the screw and the bone tunnel at 6 and 12 months postoperatively in the PLGA/β-TCP group. (D, H, L, P) At 1, 3, 6, and 12 months, as time went on, osteoid tissue and new bone appeared around the screws in the mPLA/HA group (arrows). B, bone; G, graft; S, screw; FT, fibrous tissue.

To obtain stable fixation strength to ensure enough time for tendon-bone healing,[33] clinically, the screws should keep effective fixation for ≥6 months or even >1 year.[1,18] Otherwise, it is easy to cause graft micromotion in the bone tunnel and potential TW. In this study, by choosing different ratios of L- and D-isomers ratio in PLA, we were going to realize the controllable degeneration rate of screws to meet practical clinical needs. The combination of l- and D-isomers in different ratios leads to different crystallinities of the polymer, effectively influencing water molecules to penetrate the polymer and attack the ester bonds, causing degradation.[24,29] After proportion optimization, the degradation behavior of the mPLA/HA screw is proper for the actual clinical bone healing process. Moreover, mPLA/HA screws possess ultra-high strength because of the microstructure of highly oriented alignment of polymer chains compared with PLGA/β-TCP screws. Therefore, it can be observed that the bending strength

of mPLA/HA screws during real-time degradation is always greater than that of cortical bone in young adults within 5 months (Figure 4C).

Limitations

There are some limitations to this study. First, the control screw using PLGA/β-TCP materials is only 1 of the frequently used screws for clinical application. We still need more experiments to compare the clinical effects of different screws, which may be composed of different material components. Second, due to the limitations of animal size, we could use only screws with the size of 5 × 12 mm in the experiment. Its actual biomechanical performance in vivo might be different from that in humans. But the anatomic structure of the knee joint of the beagle dog is similar to that of human beings. Nevertheless, this study systematically proves that mPLA/HA screw can ameliorate TW under the same clinical conditions.

CONCLUSION

In this study, the modified PLA/HA screw showed a special self-locking effect, satisfactory osteoinductive activity, and comparable mechanical properties compared with the PLGA/β-TCP screw. Additionally, it showed potential clinical translation possibility in terms of biomechanical properties and optimized degradation behavior. Furthermore, in the ACLR animal model, it was able to effectively ameliorate screw-bone integration and postoperative TW. The mPLA/HA screw provides a feasible option for graft fixation in ACLR.

Supplemental material for this article is available at https://journals.sagepub.com/doi/full/10.1177/23259671241271710#supplementary-materials.

REFERENCES

1. Brinlee AW, Dickenson SB, Hunter-Giordano A, Snyder-Mackler L. ACL reconstruction rehabilitation: clinical data, biologic healing, and criterion-based milestones to inform a return-to-sport guideline. *Sports Health*. 2022;14(5):770-779.
2. Buck DC, Simonian PT, Larson RV, Borrow J, Nathanson DA. Timeline of tibial tunnel expansion after single-incision hamstring anterior cruciate ligament reconstruction. *Arthroscopy*. 2004;20(1):34-36.
3. Cameron M, Buchgraber A, Passler H, et al. The natural history of the anterior cruciate ligament-deficient knee: changes in synovial fluid cytokine and keratan sulfate concentrations. *Am J Sports Med*. 1997;25(6):751-754.
4. Cameron ML, Fu FH, Paessler HH, Schneider M, Evans CH. Synovial fluid cytokine concentrations as possible prognostic indicators in the ACL-deficient knee. *Knee Surg Sports Traumatol Arthrosc*. 1994;2(1):38-44.
5. Cui L, Zhang J, Zou J, et al. Electroactive composite scaffold with locally expressed osteoinductive factor for synergistic bone repair upon electrical stimulation. *Biomaterials*. 2020;230:119617.
6. Fahey M, Indelicato PA. Bone tunnel enlargement after anterior cruciate ligament replacement. *Am J Sports Med*. 1994;22(3):410-414.
7. Fink C, Zapp M, Benedetto KP, et al. Tibial tunnel enlargement following anterior cruciate ligament reconstruction with patellar tendon autograft. *Arthroscopy*. 2001;17(2):138-143.
8. Höher J, Möller HD, Fu FH. Bone tunnel enlargement after anterior cruciate ligament reconstruction: fact or fiction? *Knee Surg Sports Traumatol Arthrosc*. 1998;6(4):231-240.
9. Huangfu X, Zhao J. Tendon-bone healing enhancement using injectable tricalcium phosphate in a dog anterior cruciate ligament reconstruction model. *Arthroscopy*. 2007;23(5):455-462.
10. Ishibashi Y, Rudy TW, Livesay GA, et al. The effect of anterior cruciate ligament graft fixation site at the tibia on knee stability: evaluation using a robotic testing system. *Arthroscopy*. 1997;13(2):177-182.
11. Jackson DW, Windler GE, Simon TM. Intraarticular reaction associated with the use of freeze-dried, ethylene oxide-sterilized bone-patella tendon-bone allografts in the reconstruction of the anterior cruciate ligament. *Am J Sports Med*. 1990;18(1):1-11.
12. Jo H, Jun DS, Lee DY, et al. Tibial tunnel area changes following arthroscopic anterior cruciate ligament reconstructions with autogenous patellar tendon graft. *Knee Surg Sports Traumatol Arthrosc*. 2004;12(4):311-316.
13. L'Insalata JC, Klatt B, Fu FH, Harner CD. Tunnel expansion following anterior cruciate ligament reconstruction: a comparison of hamstring and patellar tendon autografts. *Knee Surg Sports Traumatol Arthrosc*. 1997;5(4):234-238.
14. LaBella CR, Hennrikus W, Hewett TE. Anterior cruciate ligament injuries: diagnosis, treatment, and prevention. *Pediatrics*. 2014;133(5):e1437-e1450.
15. Lee DK, Kim JH, Lee S-S, et al. Femoral tunnel widening after double-bundle anterior cruciate ligament reconstruction with hamstring autograft produces a small shift of the tunnel position in the anterior and distal direction: computed tomography-based retrospective cohort analysis. *Arthroscopy*. 2021;37(8):2554-2563.
16. Macarini L, Murrone M, Marini S, Mocci A, Ettorre GC. MRI in ACL reconstructive surgery with PDLLA bioabsorbable interference screws: evaluation of degradation and osteointegration processes of bioabsorbable screws [Article in English, Italian]. *Radiol Med*. 2004;107(1-2):47-57.
17. Magen HE, Howell SM, Hull ML. Structural properties of six tibial fixation methods for anterior cruciate ligament soft tissue grafts. *Am J Sports Med*. 1999;27(1):35-43.
18. Muller B, Bowman KF, Bedi A. ACL graft healing and biologics. *Clin Sports Med*. 2013;32(1):93-109.
19. National Research Council (US) Committee for the Update of the Guide for the Care and Use of Laboratory Animals. Guide for the Care and Use of Laboratory Animals. 8th ed. Washington (DC): National Academies Press (US); 2011.
20. Padilla S, Benito-Garzón L, Enciso Sanz S, et al. Novel osteoinductive and osteogenic scaffolds of monetite, amorphous calcium phosphate, hydroxyapatite, and silica gel: influence of the hydroxyapatite/monetite ratio on their behavior and on their physical and chemical properties. *ACS Biomater Sci Eng*. 2020;6(6):3440-3453.
21. Roberts TS, Drez D, McCarthy W, Paine R. Anterior cruciate ligament reconstruction using freeze-dried, ethylene oxide-sterilized, bone-patellar tendon-bone allografts: two year results in thirty-six patients. *Am J Sports Med*. 1991;19(1):35-41.
22. Schmalzried TP, Akizuki KH, Fedenko AN, Mirra J. The role of access of joint fluid to bone in periarticular osteolysis: a report of four cases. *J Bone Joint Surg Am*. 1997;79(3):447-452.
23. Seil R, Rupp S, Krauss PW, Benz A, Kohn DM. Comparison of initial fixation strength between biodegradable and metallic interference screws and a press-fit fixation technique in a porcine model. *Am J Sports Med*. 1998;26(6):815-819.
24. Serizawa T, Arikawa Y, Hamada K, et al. Alkaline hydrolysis of enantiomeric poly(lactide)s stereocomplex deposited on solid substrates. *Macromolecules*. 2003;36(6):1762-1765.
25. Shellock FG, Mink JH, Curtin S, Friedman MJ. MR imaging and metallic implants for anterior cruciate ligament reconstruction: assessment of ferromagnetism and artifact. *J Magn Reson Imaging*. 1992;2(2):225-228.

26. Singhatat W, Lawhorn KW, Howell SM, Hull ML. How four weeks of implantation affect the strength and stiffness of a tendon graft in a bone tunnel: a study of two fixation devices in an extraarticular model in ovine. *Am J Sports Med*. 2002;30(4):506-513.
27. Surer L, Yapici C, Guglielmino C, et al. Fibrin clot prevents bone tunnel enlargement after ACL reconstruction with allograft. *Knee Surg Sports Traumatol Arthrosc*. 2017;25(5):1555-1560.
28. Taketomi S. Editorial commentary: tunnel widening after anterior cruciate ligament reconstruction may increase laxity and complicate revision. *Arthroscopy*. 2021;37(8):2564-2566.
29. Tsuji H. In vitro hydrolysis of blends from enantiomeric poly(lactide)s part 1. Well-stereo-complexed blend and non-blended films. *Polymer*. 2000;41(10):3621-3630.
30. Wang H, Zhang B, Cheng C-K. Stiffness and shape of the ACL graft affects tunnel enlargement and graft wear. *Knee Surg Sports Traumatol Arthrosc*. 2020;28(7):2184-2193.
31. Wilson TC, Kantaras A, Atay A, Johnson DL. Tunnel enlargement after anterior cruciate ligament surgery. *Am J Sports Med*. 2004;32(2):543-549.
32. Wolfson TS, Mannino B, Owens BD, Waterman BR, Alaia MJ. Tunnel management in revision anterior cruciate ligament reconstruction: current concepts. *Am J Sports Med*. 2023;51(2):545-556.
33. Yao SY, Cao MD, He X, Fu BSC, Yung PSH. Biological modulations to facilitate graft healing in anterior cruciate ligament reconstruction (ACLR), when and where to apply? A systematic review. *J Orthop Translat*. 2021;30:51-60.
34. Yue L, DeFroda SF, Sullivan K, Garcia D, Owens BD. Mechanisms of bone tunnel enlargement following anterior cruciate ligament reconstruction. *JBJS Rev*. 2020;8(4):e0120.
35. Zantop T, Weimann A, Schmidtko R, et al. Graft laceration and pull-out strength of soft-tissue anterior cruciate ligament reconstruction: in vitro study comparing titanium, poly-d,l-lactide, and poly-d,l-lactide-tricalcium phosphate screws. *Arthroscopy*. 2006;22(11):1204-1210.
36. Zhang T, Yan S, Song Y, et al. Exosomes secreted by hypoxia-stimulated bone-marrow mesenchymal stem cells promote grafted tendon-bone tunnel healing in rat anterior cruciate ligament reconstruction model. *J Orthop Translat*. 2022;36:152-163.
37. Zhao L, Zhao J, Yu J-J, Zhang C. Irregular bone defect repair using tissue-engineered periosteum in a rabbit model. *Tissue Eng Regen Med*. 2020;17(5):717-727.
38. Zhao R, Xie P, Zhang K, et al. Selective effect of hydroxyapatite nanoparticles on osteoporotic and healthy bone formation correlates with intracellular calcium homeostasis regulation. *Acta Biomater*. 2017;59:338-350.
39. Zhu B, Xu W, Liu J, Ding J, Chen X. Osteoinductive agents-incorporated three-dimensional biphasic polymer scaffold for synergistic bone regeneration. *ACS Biomater Sci Eng*. 2019;5(2):986-995.